Intrinsic losses in self-assembled hybrid metallodielectric systems

J. F. Galisteo-López,[1,a)] M. López-García,[1] C. López,[1] and A. García-Martín[2]
[1]*Instituto de Ciencia de Materiales de Madrid (CSIC) and Unidad Asociada CSIC-U. Vigo, C/Sor Juana Inés de la Cruz 3, 28049 Madrid, Spain*
[2]*IMM-Instituto de Microelectrónica de Madrid (CNM-CSIC), c/Isaac Newton 8, PTM, Tres Cantos, 28760 Madrid, Spain*

(Received 5 May 2011; accepted 28 July 2011; published online 22 August 2011)

The light confinement properties of hybrid metallodielectric systems have been studied employing numerical simulations to obtain the optical response as well as the total field intensity associated with the different modes of the structure. The effect of intrinsic losses, absorption, and out-of-plane leakage on the quality factors (Q) of different modes is discussed, and the results obtained are interpreted in terms of the optical constants of the metallic substrate. Large Q values (up to 600) can be attained in this kind of samples, much larger than in their purely dielectric counterpart, pointing to the ability of these systems to efficiently confine electromagnetic radiation. © *2011 American Institute of Physics*. [doi:10.1063/1.3626856]

The last two decades have witnessed a growing interest in self-assembly techniques as a straightforward and low-cost approach to fabricate photonic structures.[1] Perhaps the most widespread example is that of artificial opals, arguably the most popular approach to fabricate three-dimensional (3D) photonic crystals (PhC).[2] But lower dimensionality 2D structures have also been explored in a number of fields where they could find applications such as inexpensive lithography masks,[3] microlens arrays,[4] or templates to fabricate complex plasmonic architectures[5] with potential use as surface enhanced Raman spectroscopy (SERS) substrates.[6] Recently, a renewed interest in 2D arrays made from dielectric colloids has arisen as a route to fabricate hybrid metallodielectric systems where a periodic dielectric lattice is coupled to a surface plasmon polariton (SPP) supporting metallic substrate. In these systems, the combination of a dielectric periodicity and a metallic interface causes a strong spatial redistribution of the electromagnetic (EM) field which can yield to large field enhancements not attainable in the purely dielectric counterpart.[7,8] This is caused by the development of modes where the EM field is mainly located within the dielectric spheres, in close vicinity to the metallic surface or in both regions. The possibility to use these systems as a means to strongly modify the spontaneous emission of internal sources[8] or as sensitive chemical sensors[9] has been recently proposed and experimentally demonstrated.

When envisioning an actual application using this kind of systems, it is crucial to care not only about the ability of the structure to provide spatial field confinement but also on the efficiency with which it will confine light. Losses, present in any real world fabricated sample, are responsible for a poor confinement which could render the sample useless for certain applications.[10] For the system under consideration in the present work, the sources of losses can be divided into extrinsic, associated with structural imperfections appearing during the growth process, and intrinsic ones. The latter is characteristic of an ideal, perfectly ordered sample and can be attributed to two distinct sources: (1) out-of-plane radiative losses due to energy leakage from the sample to the air/substrate and (2) absorption losses originating from the presence of an absorptive metal substrate.

In the present work, we are interested in studying the effect of intrinsic losses on the different types of modes present in hybrid systems, paying special attention to its efficiency in confining EM radiation. In particular, we will study, using a numerical approach, a model system consisting of periodic 2D hexagonal close-packed arrays of polystyrene (PS) spheres deposited on gold substrates, a configuration which has been studied over the past years[7–9,11] and has shown to be effective in enhancing light-matter interaction. The optical response of samples having an increasing sphere diameter but identical substrate has been obtained, together with the spatial distribution of the total field intensity associated with the different modes present in the system, by means of finite difference time domain (FDTD) simulations.[12] A fine grid ($\geq$ 40 points per wavelength in each direction) together with sufficiently long simulation times ($\geq$ 1 ps) was used in order to account for the presence of the metal substrate and the possibility of coupling to resonant modes. The optical constants used for the metal substrates were obtained experimentally from ellipsometric measurements. Increasing the sphere diameter shifts the spectral position of the different modes of the system so that we can retrieve the quality (Q) factor at each step and obtain the chromatic dispersion of the losses.

Figure 1 shows the calculated normal incidence reflection spectra for monolayers of PS spheres with 450 and 750 nm diameters together with the total field intensity associated with the three modes for the 750 nm case in the spectral range under consideration. For the latter diameter, such modes appear as sharp dips over a nearly 100% reflectance background coming from the gold substrate. For the case of the smaller spheres, a monotonic decrease in the background reflectance takes place for wavelengths below $\lambda \sim 650$ nm, due to the onset of absorption by the metallic substrate, which hampers the observation of the modes of the system. Depending on the spatial distribution of the field pattern, the modes of the system can be divided between SPP-like (G1 and G3) with most of the field intensity located at the metal surface and waveguided

a)Electronic mail: galisteo@icmm.csic.es.

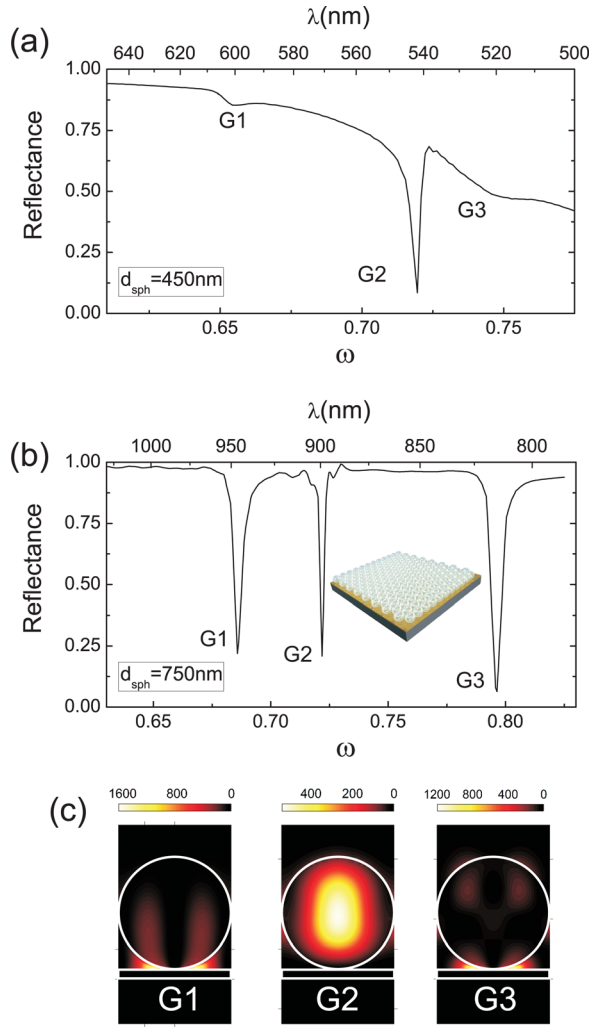

FIG. 1. (Color online) (a) Reflection spectra from monolayers of PS spheres deposited on a gold substrate having 450 nm (a) and 750 nm (b) diameters. Inset shows a diagram of the sample; (c) shows total field intensity distribution for the latter case.

(WG)-like (G2) with most of the field intensity located within the dielectric sphere. For those frequencies corresponding to the different modes, field enhancements of several orders of magnitude can be observed, evidencing the ability of this type of structures to enhance light matter interaction.

It is also important to analyse the spectral position of the three types of modes as the sphere diameter varies (we have considered the range 450-1250 nm in steps of 100 nm). Figure 2(a) contains the spectral position of the three modes, showing that each mode follows a linear trend and with the present diameter range the system modes can be shifted from $\lambda = 600$ nm up to 1500 nm. Should the visible range below 600 nm be preferred, a substrate of a different nature, such as silver, would be more appropriate as absorption begins at shorter wavelengths. In order to reproduce the spectral position of the two different types of modes, we can use an empty lattice model in which the dispersion relation of a lossless dielectric (G2) or an SPP (G1, G3) is folded in reciprocal space according to the periodicity of the lattice. For G2, we use $2\pi n_{eff}/\lambda = |\boldsymbol{k}| = |\boldsymbol{G}|$, $\mathbf{G}$ being the shortest reciprocal lattice vector ($\frac{4\pi}{\sqrt{3}} d_{sph}$, where d_{sph} is the sphere diameter) and n_{eff} is an effective refractive index which in our case is 1.38, matching the average refractive index resulting from

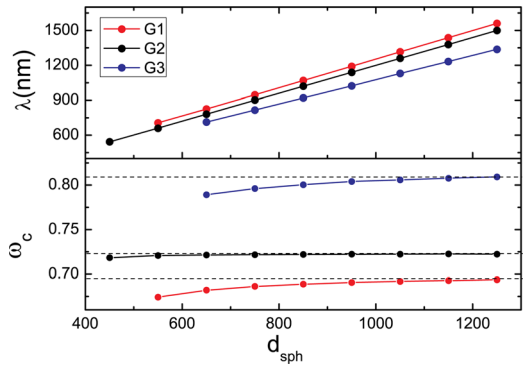

FIG. 2. (Color online) Spectral position of the G1, G2, and G3 modes for samples with increasing sphere diameter as a function of wavelength (top) and reduced frequency ω_c (bottom).

weighting the filling fraction of polymer and air in the monolayer. For G1 and G3, we assume the typical SPP dispersion relation and fold it similarly: $2\pi\sqrt{\frac{\varepsilon_1\varepsilon_2}{\varepsilon_1+\varepsilon_2}}/\lambda = |\boldsymbol{k}| = |\boldsymbol{G}|$, where ε_1 and ε_2 are the real components of the dielectric constants of metal and dielectric on which the SPP propagates. To reproduce the results for G1 and G3, we must use $\varepsilon_2 = 1.44$ and 1.27, respectively. This difference in refractive index only confirms the fact that the total field intensity is distributed between air and PS differently for the G1 and G3 modes.

Figure 2(b) shows the same data in terms of a reduced frequency $\omega = \sqrt{3} d_{sph}/2\lambda$, where λ is the wavelength of light in vacuum. This sort of plot helps highlighting the departure from scalability. Modes whose frequency scales with size like in PhCs show a constant ω_c in this plot, whereas modes that depart from scalability due to the dispersion of the materials involved present a frequency shift.[13] This behaviour can be explained by the total field intensity being strongly localized within the sphere volume, as for the G2 mode, and hence not being able to sense the dispersive elements present in the structure, i.e., the metal substrate. On the other hand, modes G1 and G3 are strongly sensitive to the optical nature of the substrate as most of their field intensity is located in its close vicinity. Therefore, it is expected that their spectral position will be strongly dispersive. We will come back to this point later in this Letter.

In order to explore the losses of the different modes, we have extracted the Q factor associated with each of them which gives us the efficiency with which they confine light. When referring to an optical cavity, the Q of the cavity modes gives the ratio between the energy stored in the cavity to the energy lost per cycle and is proportional to the characteristic time of the exponential decay of stored energy. Analogously, for the case of a perfectly periodic 2D PhC, Q is also a measure of the confinement of energy in a given mode; however, contrary to the case of the microcavity, where energy is located within the cavity volume, here energy is distributed throughout the crystal volume. The quality factor $Q = \Delta\omega/\omega_c$ can be obtained from the calculated reflectance spectra, such as the one shown in Figure 1, $\Delta\omega$ being the full width at half maximum (FWHM) of each mode and ω_c its spectral position.

Figure 3(a) shows the evolution as a function of wavelength of the Q of each of the three modes considered. In order to change the spectral position of each mode we increased the

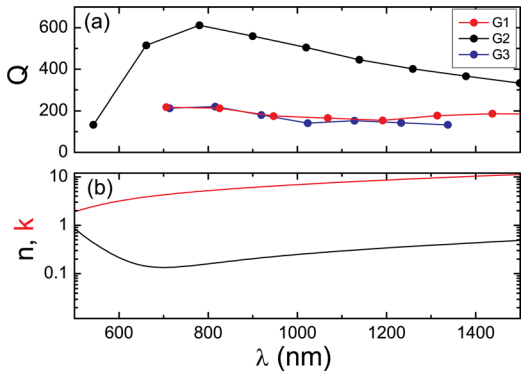

FIG. 3. (Color online) (a) Quality factors (Q) of the different modes of the system as a function of wavelength. (b) Optical constants of gold substrate.

sphere diameter. Each point in the figure corresponds to a sphere diameter which for G2 covers the whole 450-1250 nm range while for G1 and G3 results could only be obtained for the 550-1250 nm and 650-1250 nm intervals, respectively. For smaller diameters, the latter modes fall in the spectral region where the gold substrate strongly absorbs, which hampers their observation as evidenced in Fig. 1(a). We can see how G2 undergoes a strong variation as its frequency is shifted, with a maximum close to 750 nm, while G1 and G3 hardly change in the same spectral range. Regarding the absolute values of Q obtained, we can see how in the case of G2 a Q of up to 600 can be achieved for $d_{sph} = 650$ nm spheres. These values, though not as large as those attainable in 2D slab PhC, are much larger than those which can be obtained in configurations where dielectric substrates are employed, even for the ideal case of a free standing monolayer (ca. 100) where leakage to the substrate is minimized. For the case of G1 and G3, large values can be obtained up to 220, two-fold larger than those reported for similar systems.[9]

In order to understand these results, we have compared the evolution of the calculated quality factors with the optical constants of the gold substrate (which have been obtained from ellipsometric measurements on thin films deposited by sputtering—see Figure 3(b)). For the case of G2, the evolution of Q is clearly correlated with the real part of the refractive index of gold (n). Due to the fact that the field intensity for this mode is concentrated within the dielectric spheres, (see Figure 1) intrinsic losses will be mainly due to energy leakage to the environment with little contribution from absorption by the metal. Radiative losses are governed by the real component of the refractive index of the environment as light confinement is due to total reflection in the vertical direction and to Bragg diffraction in the plane of the periodicity. In order to obtain light confinement within the monolayer, one needs a refractive index lower than the effective index of the periodic dielectric array, ca. 1.38. In the spectral range under consideration, n of gold is always below 1, and hence the confinement obtained is superior to the case of the free-standing monolayer (surrounded by vacuum) with a maximum near $\lambda = 750$ nm where $n = 0.1$.

Finally, we consider the confinement for G1 and G3, where part of the total field intensity is located close to the metal surface. In this case both Q have similar values which oscillate between 220 and 130 depending on the dielectric sphere diameter considered. In principle, for these modes, losses are due both to out-of-plane radiative losses and absorption, where the contributions of one or the other will be dependent on the way the field intensity is distributed. But the fact that the values obtained are much lower than those obtained for G2 indicates that absorption is likely to be the dominant source of losses. Returning to the dispersion in the spectral position of the modes presented in Figure 2 and comparing it with the optical constants of the gold substrate, we can see how the spectral evolution of the G1 and G3 modes follow a trend similar to that of the imaginary component of the substrate refractive index (k). As mentioned above, these modes should be more sensitive to the dispersion of the gold substrate as a significant part of their field intensity is located in close vicinity to the metal interface.

In conclusion, we have studied the light confinement properties of hybrid metallodielectric systems consisting of self-assembled 2D arrays of dielectric spheres coupled to SPP supporting substrates. The chromatic dispersion of the Q factor of the different types of modes present in this kind of sample has been observed to be strongly dependent on the optical constants of the metal substrate. Q factors up to 600, much larger than those attainable in similar systems with dielectric substrates and free-standing configurations, can be obtained by choosing the appropriate sphere diameter. The combination of such optical performances with a straightforward fabrication process could make the use of these systems interesting in a number of applications such as photovoltaic cells as recently proposed.[14]

J. F. Galisteo-López was supported by the JAE Postdoctoral Program from CSIC. M. López-García was supported by the FPI PhD program from the MICINN. This work was supported by the Spanish MICINN CSD2007-0046 (Nanolight.es) and MAT2009-07841 (GLUSFA) projects and Comunidad de Madrid S2009/MAT-1756 (PHAMA) programme. A. García-Martín also acknowledges financial support from the Spanish MICINN ("MAGPLAS" MAT2008-06765-C02-01/NAN, Funcoat Consolider Ingenio 2010 CSD2008-00023) and European Comission (NMP3-SL-2008-214107-Nanomagma).

[1]J. F. Galisteo-López, M. Ibisate, R. Sapienza, L. S. Froufe-Pérez, A. Blanco, and C. López, Adv. Mater. **23**, 30 (2011).
[2]E. Yablonovitch, Phys. Rev. Lett. **58**, 2085 (1987).
[3]Y. Li, W. Cai, and G. Duan, Chem. Mater. **20**, 615 (2008).
[4]P. Kumnorkaew, Y.-K. Ee, N. Tansu, and J. F. Gilchrist, Langmuir **24**, 12150 (2008).
[5]R. M. Cole, Y. Sugawara, J. J. Baumberg, S. Mahajan, M. E. Abdelsalam, and P. N. Barlett, Phys. Rev. Lett. **97**, 137401 (2006).
[6]Y.-J. Oh, S.-G. Park, M.-H. Kang, J.-H. Choi, Y. Nam, and K.-H. Jeong, Small **7**, 184 (2011).
[7]L. Shi, X. Liu, H. Yin, and J. Zi, Phys. Lett. A **37**, 1059 (2010).
[8]M. López-García, J. F. Galisteo-López, A. Blanco, J. Sánchez-Marcos, C. López, and A. García-Martín, Small **6**, 1757 (2010).
[9]X. Yu, L. Shi, D. Han, J. Zi, and P. V. Braun, Adv. Funct. Mater. **20**, 1910 (2010).
[10]J. Grandidier, S. Massenot, G. Colas des Francs, A. Bouhelier, J.-C. Weeber, L. Markey, A. Dereux, J. Renger, M. U. González, and R. Quidant, Phys. Rev. B **78**, 245419 (2008).
[11]M. López-García, J. F. Galisteo-López, A. Blanco, C. López, and A. García-Martín, Adv. Funct. Mater. **20**, 4338 (2010).
[12]Numerical simulations were performed with a commercial software (Lumerical FDTD Solutions).
[13]K. Sakoda, *Optical Properties of Photonic Crystals* (Springer, Berlin, 2001).
[14]J. Grandidier, D. M. Callahan, J. N. Munday, and H. A. Atwater, Adv. Mater. **23**, 1171 (2011).